



**Applicability of new degradable hypericin-polymer-conjugates as photosensitizers: principle mode of action demonstrated by in-vitro models**

Journal:	<i>Photochemical &amp; Photobiological Sciences</i>
Manuscript ID:	PP-ART-07-2014-000251.R1
Article Type:	Paper
Date Submitted by the Author:	01-Sep-2014
Complete List of Authors:	Feinweber, Daniela; University of Salzburg, Department of Molecular Biology Verwanger, Thomas; University of Salzburg, Department of Molecular Biology Brueggemann, Oliver; Johannes Kepler University Linz, Institute of Polymer Chemistry Teasdale, Ian; Johannes Kepler University Linz, Institute of Polymer Chemistry Krammer, Barbara; University of Salzburg, Department of Molecular Biology

## Applicability of new degradable hypericin-polymer-conjugates as photosensitizers: principle mode of action demonstrated by *in-vitro* models

Daniela Feinweber<sup>a</sup>, Thomas Verwanger<sup>a</sup>, Oliver Brüggemann<sup>b</sup>, Ian Teasdale<sup>b</sup> and Barbara Krammer<sup>a,\*</sup>

<sup>a</sup> Division of Molecular Tumor Biology, Department of Molecular Biology, University of Salzburg, Hellbrunnerstrasse 34, 5020 Salzburg, Austria

<sup>b</sup> Institute of Polymer Chemistry, Johannes Kepler University Linz, Welser Strasse 42, 4060 Leonding, Austria

\* Corresponding author: Dr Barbara Krammer, Division of Molecular Tumor Biology, Department of Molecular Biology, University of Salzburg, Hellbrunnerstrasse 34, 5020 Salzburg, Austria; Phone: ++43-662-8044-5703; email: barbara.krammer@sbg.ac.at

Two series of water soluble novel conjugates of the photosensitizer hypericin were prepared and evaluated for their use as agents for photodynamic therapy, with covalently and non-covalently loaded hypericin based on functionalised, hydrolytically degradable inorganic-organic hybrid polyphosphazenes. The conjugates showed excellent aqueous solubility and similar fluorescence spectra to pristine hypericin. Detailed *in-vitro* investigations revealed that the substances were non-toxic in the dark over a wide concentration range, but displayed phototoxicity upon irradiation. Cell uptake studies showed rapid uptake with localization of hypericin observed in endoplasmic reticulum, Golgi complex and particularly in the lysosomes. Furthermore, a DNA fragmentation assay revealed that the photosensitizer conjugates are efficient inducers of apoptosis with some tumor cell selectivity caused by faster and enhanced accumulation in A431 than in HaCaT cells, and thus a moderately higher phototoxicity of A431 compared to HaCaT cells. These novel photosensitizer conjugates hence represent viable hydrolytically degradable alternatives for the advanced delivery of hypericin.

### 1. Introduction

Fluorescence diagnosis (FD) and photodynamic therapy (PDT) of flat lesions using hypericin as photosensitizer have shown very promising results<sup>1</sup>. Hypericin (Hyp), a constituent of St. John's wort, exhibits a bright fluorescence and many features of an optimal photosensitizer: it accumulates rapidly in cells, localizing mainly in the endoplasmic reticulum (ER), Golgi apparatus and lysosomes<sup>1</sup>; it generates singlet oxygen efficiently upon irradiation, inducing high phototoxicity which, depending on drug and light doses, results in apoptosis or necrosis, as well as triggering immune responses. Hyp has shown tumor selectivity in diagnosis and therapy<sup>2-10</sup>. Furthermore, Hyp is applied also as an antibacterial<sup>11</sup> or antiviral agent<sup>12,13</sup>, and it is able to modulate signaling pathways<sup>14</sup>.

Since hypericin as its monobasic salt is essentially non-water soluble under physiological conditions, carriers and solubility enhancers such as nanoparticles<sup>15</sup>, PEG (polyethyleneglycol)<sup>16</sup>, liposomes<sup>8,17</sup> or PVP (polyvinyl pyrrolidone)<sup>18</sup> are required to enable administration and to prevent fluorescence/ efficiency quenching by aggregation of the

photosensitizer prior to delivery to the cells in vitro or to the tissue in vivo<sup>8,19</sup>. PVP formulations with Hyp provide a simple and highly effective administration<sup>20</sup>, and indeed PVP-hypericin is currently in the approval process for diagnosis of bladder cancer<sup>18</sup>. In addition, PVP-hypericin shows phototoxicity and tumor selectivity in vivo with a higher accumulation in malignant than in normal rat urothelium<sup>21</sup> and in spheroids of malignant and normal human urothelial cells<sup>22</sup>. However, long-term use of non-degradable polymers at  $M_w$  above the renal clearance limit is problematic due to the risk of lysosomal accumulation<sup>23-25</sup> and reported liver cell vacuolation<sup>26</sup>. Indeed PVP with  $M_w$  above 10 kDa is not recommended for repeated use in preparations which could lead to excessive storage in the body<sup>27,28</sup>. Since high  $M_w$  is the desired property required for pharmacokinetic enhancement with most polymer formulations (including PVP-hypericin<sup>20</sup>) it becomes clear, that the search for alternative conjugates or delivery vehicles for photosensitizers is of primary interest.

Poly(organo)phosphazenes, a relatively unique group of inorganic-organic hybrid polymers consisting of a repeating phosphorus, nitrogen backbone with organic side groups, have many properties ideally suited to biomedical applications<sup>29-31</sup>. These properties include controllable molecular dimensions<sup>32</sup> and tunable rates of (bio)degradation<sup>29</sup>. The degradation products of these polymers are usually non-toxic, consisting of phosphates, ammonia and the corresponding side groups<sup>29</sup>. The aim of the study was therefore to design and synthesize novel non-covalently and covalently bound hydrolytically degradable, polyphosphazene based<sup>31,33,34</sup> drug carriers and solubility enhancers for coupling to Hyp and to test these constructs for use as photosensitizer conjugates in human non-malignant and malignant dermal cell lines. A comparison of these new materials is also made to the previously reported conjugate PVP-hypericin.

## 2. Experimental section

### 2.1 Polymer synthesis and conjugation with hypericin

Hypericin was prepared using methods reported by Falk et al.<sup>35</sup>. The synthetic procedure for polydi[2-(2-oxo-1-pyrrolidinyloxy)phosphazene]<sup>29</sup> (PYRP) was adapted from literature methods<sup>36</sup>. Firstly, polydichlorophosphazene ( $n=50$ ) was prepared by the living cationic polymerization of  $\text{Cl}_3\text{PNTMS}$  in the presence of  $\text{PCl}_5$ <sup>32</sup>. Separately, under argon, NaH (267 mg, 6.8 mmol) was suspended in anhydrous THF (30 mL) and a large excess of 1-(2-hydroxyethyl)-2-pyrrolidone (4.31 g, 31.1 mmol) was added. After 1.5 hours the polydichlorophosphazene precursor (258 mg, 2.2 mmol), dissolved in 5 mL THF was added. The reaction was stirred at room temperature for 16 h. The precipitating salts were filtered, the polymer precipitated in diethyl ether and then purified by dialysis against  $\text{H}_2\text{O}$  (48 h) and ethanol (24 h). Yield 360 mg (53 %).  $^1\text{H}$  NMR (300 MHz,  $\text{CDCl}_3$ ,  $\delta$ ): 4.03 (br, 2H), 3.49 (br, 4H), 2.32 (br, 2H), 20.3 (br, 2H) ppm;  $^{31}\text{P}$  NMR (121 MHz,  $\text{CDCl}_3$ ,  $\delta$ ): -8.2 ppm; SEC:  $M_n = 17\,600\text{ g mol}^{-1}$ ,  $M_w / M_n = 1.1$

Non-covalent conjugates were then prepared from PYRP as follows: Hypericin (2.4 mg,  $4.8 \times 10^{-3}$  mmol) was dissolved in abs. ethanol (2 mL). After dissolution, the solution was poured onto PYRP (200 mg). The solvents were then removed under vacuum to give the conjugate HypPYRP in quantitative yield. The conjugate HypPVP was prepared in an analogous manner, using PVP40 as purchased from Sigma Aldrich.

Additionally, hypericin is covalently bound to a JFMP polymer, which entails a Jeffamine (polyethylene oxide-co-poly-propylene oxide-NH<sub>2</sub>) grafted polyphosphazene. HypJFMP\_1, 2 and 3 were prepared as previously reported<sup>38</sup> with the required amount of hypericin adjusted accordingly.

A summary of the Hyp-conjugates and the respective pristine polymers tested is provided in table 1.

**Table 1.** Summary of the Hyp-conjugates and pristine polymer series tested

Sample	Description	M <sub>w</sub> (approx) / kDa	% wt Hypericin
HypPYRP	Pyrrolidone functionalized polyphosphazene (PYRP) with non-covalently bound hypericin	20	1.20
HypPVP	Polyvinylpyrrolidone with non-covalently bound hypericin	40	1.18
PYRP	Pristine polymer PYRP	20	0
PVP	Pristine polymer PVP	40	0
HypJFMP_1	Jeffamine-NH <sub>2</sub> (2kDa) grafted polyphosphazene with covalently bound hypericin	200	0.7
HypJFMP_2	Jeffamine-NH <sub>2</sub> (2kDa) grafted polyphosphazene with covalently bound hypericin	200	1.6
HypJFMP_3	Jeffamine-NH <sub>2</sub> (1kDa) grafted polyphosphazene with covalently bound hypericin	100	3.4
JFMP	Jeffamine-NH <sub>2</sub> (1kDa) grafted polyphosphazene	100	0

## 2.2. Fluorescence spectrophotometry

Emission and excitation spectra of hypericin conjugates were recorded by a fluorescence spectrophotometer (Hitachi F-4500, Inula, Vienna, Austria). The emission spectra were excited with the second highest excitation peak at about 555 nm in order to avoid peak overlapping due to Rayleigh scattering.

## 2.3. Cells and cell culture

Human squamous cell carcinoma cell line, A431 (ATCC-Nr. CRL-1555), human p53-deficient keratinocytes, HaCaT, and primary human dermal fibroblasts were used for the study. Cells were cultivated in Dulbecco's modified Eagle's medium (DMEM) supplemented with 1M HEPES Buffer, 5 % (A431) or 10 % (HaCaT, dermal fibroblasts) fetal bovine serum (FBS), 4 mM, L-glutamine, 1 mM Na-pyruvate, 100 U/ml penicillin and 0.1 mg/ml streptomycin. All media and supplements were obtained from PAA (Pasching, Austria). Cells were grown at 37 °C and 5 % CO<sub>2</sub> in a humidified atmosphere; all experiments were performed using cell numbers between 15 000 and 20 000 in 96-well plates, 800 000 in 60 mm petri dishes for fluorescence microscopy or 300 000 in 35 mm dishes for cell cycle and apoptosis analysis.

## 2.4. Photodynamic treatment

For determination of the phototoxic effects of the conjugates, cells were treated with a standard PDT protocol: after incubation of seeded cells overnight, the supernatant was

carefully aspirated and replaced by 100  $\mu\text{l}$  of DMEM without serum (MOS) containing 5  $\mu\text{M}$  of the conjugate. In general, concentrations are related to the effective concentration of the photoactive substance. Cells were first incubated in the dark for 3 hours, after incubation, the medium was removed and replaced by an equal volume of the respective medium with serum. Irradiation was performed from the bottom of the culture receptacle with a red-light diode array ( $\lambda_{\text{max}} = 610 \pm 10 \text{ nm}$ ; power density = 1.8  $\text{mW}/\text{cm}^2$ ; super bright diodes, product No. L53SRC-F, Kingbright Electronic, Issum, Germany) for different time periods. Afterwards, cells were incubated in the dark.

### **2.5. Dark and phototoxicity**

Cytotoxicity ("dark toxicity") of the conjugates was measured under dark conditions (without irradiation and handling under subdued light conditions). For this purpose, 24 hours after seeding the cells, the supernatant was carefully removed and replaced with 100  $\mu\text{l}$  of MOS containing increasing photosensitizer (PS) concentrations (1  $\mu\text{M}$  up to 80  $\mu\text{M}$ ). After three hours of incubation, MOS containing the PS was removed and replaced with DMEM with either 5 % or 10 % FBS. Cells were then incubated for another 24 hours. Two different controls, one at the beginning of the incubation ( $C_0$ ) and one after incubation for another 24 hours ( $C_{24}$ ) were included to determine proliferative (values  $> C_{24}$ ), cytostatic (values  $> C_0$  and  $< C_{24}$ ) or cytotoxic (values  $< C_0$ ) effects of the conjugates.

Phototoxicity of the conjugates was measured 24 h after irradiation with different irradiation times, as described in 2.4. In order to achieve similar dose-effect curves for each photosensitizer-conjugate the photosensitizing dose (sensitizer x irradiation) was adapted by different irradiation times and therefore different fluences while using the same photosensitizer concentration of 5  $\mu\text{M}$ .

Pristine polymers were also measured concerning their dark and phototoxicity. Indications of the polymer concentrations refer to the corresponding molarity of the hypericin conjugates, which in turn derives from the effective concentration of the photoactive substance.

MTT assays were performed to measure mitochondrial activity indicating viable cells by means of reduction of yellow 3-[4,5-dimethylthiazolyl]-2,5-diphenyltetrazolium bromide (MTT) to the insoluble blue formazan catalyzed by mitochondrial and other cellular dehydrogenases. It was carried out by the addition of 10  $\mu\text{l}$  MTT solution (5  $\text{mg}/\text{ml}$  in PBS; Sigma-Aldrich, Steinheim, Germany) to the microplate wells. Reduction of MTT was allowed to proceed for 45 min at 37  $^\circ\text{C}$ . Afterwards, the medium was removed and the formazan dye was solubilized by the addition of 100  $\mu\text{l}$  iso-propyl alcohol (VWR International S.A.S., Fontenay-sous-Bois, France). The absorption was measured at 565 nm using a microplate reader (Infinite M200Pro, Tecan, Groedig, Austria). Quantitative changes of the absorption stand for changes in the viability.

For calculation of the photosensitizing efficiency, two consecutive irradiation times were chosen, one inducing more and one less than 50 % surviving cells. A line of best fit was calculated between these two data points and linear equations of these lines were used to calculate the irradiation time resulting in exactly 50 % viability.

### **2.6. Uptake kinetics**

The characteristics of the cellular uptake of the hypericin **in the** conjugates were studied by cell lysis and subsequent determination of the fluorescence signal emitted by hypericin. For

this purpose, the supernatant was carefully aspirated at different time points and replaced with 100  $\mu$ l of MOS containing 5  $\mu$ M of the photoactive substance. After incubation of the PS in the dark for up to 7 hours, the medium was aspirated and cells were washed twice with 100  $\mu$ l of PBS. After removal of the phosphate buffer, the cells were lysed for 10 min at room temperature with 50  $\mu$ l 3 % Triton X-100 (Roth, Karlsruhe, Germany) in PBS. The fluorescence of hypericin was recorded at  $\lambda_{Ex}$  = 340 nm and  $\lambda_{Em}$  = 604 nm, using an Infinite M200Pro microplate reader (Tecan, Groedig, Austria).

In order to correct for variations in the cell number seeded, the BCA assay (Pierce, Rockford, USA) was employed to determine the overall protein content of each sample. For this, 150  $\mu$ l BCA assay solution containing 49 parts BCA reagent (Pierce, Rockford, USA) and 1 part  $CuSO_4$  (4 % w/v in  $H_2O$ ; Sigma-Aldrich, Steinheim, Germany) were added to each well after fluorescence measurements. Following an incubation time of 30 min at 37 °C, the absorbance was measured at 565 nm using an Infinite M200Pro microplate reader (Tecan, Groedig, Austria).

### **2.7. Localisation**

24 hours after seeding dermal fibroblasts into 60 mm dishes (Sarstedt, Newton, USA) with cover slips, the cover slips with the attached cells were placed into 60 mm dishes with a hole allowing for high magnification fluorescence microscopy. Cells were then covered with MOS supplemented with 5  $\mu$ M PS. After an incubation time of 3 hours **with the conjugates**, microscopy was carried out by means of an inverted fluorescence microscope (Olympus IX70, Vienna, Austria) using 1000x magnification oil-immersion (filter:  $\lambda_{Ex}$  = 480 - 500 nm and  $\lambda_{Em}$  > 570 nm). **Fluorescence images of hypericin** were recorded with an F-View II CCD digital camera (Soft Imaging System GmbH, Muenster, Germany).

### **2.8. Cell cycle analysis and apoptosis detection (sub $G_1$ -assay)**

After incubation of seeded cells overnight in 35 mm dishes (Sarstedt, Newton, USA), the supernatant was aspirated and replaced by 2 ml of MOS containing 5  $\mu$ M PS. Cells were then incubated in the dark for 3 hours. Irradiation was performed from below the culture dishes with the irradiation set-up as described above in 2.4.

Cells were harvested 8 hours post irradiation: the supernatant was transferred to centrifugation tubes and the remaining cells were detached by adding 750  $\mu$ l accutase (PAA Laboratories GmbH, Pasching, Austria). Afterwards, the cells were transferred to centrifugation tubes and the suspension was centrifuged at 2 000 rpm for 3 min. Subsequently, the supernatant was removed and the cells were re-suspended in 200  $\mu$ l PBS. Cells were fixed by addition of 2 ml ice-cold 70% ethanol (Merck, Darmstadt, Germany) and incubated overnight at -20 °C. Following a further centrifugation at 2 000 rpm for 5 min, the supernatant was removed and the cells were resuspended and stained within 500  $\mu$ l of a solution containing 400  $\mu$ l PBS, 50  $\mu$ l RNase solution (1 mg/ml, Sigma-Aldrich, Steinheim, Germany) and 50  $\mu$ l propidium iodide (PI) solution (0.4 mg/ml, Biotium, Hayward, USA) for 30 min at 37 °C in the dark. Cells were then transferred to FACS tubes (BD Biosciences, Schwechat, Austria).

Fluorescence of PI was analyzed in 10 000 cells by flow cytometry (BD FACSCantoTM II Flow Cytometer, BD Biosciences, Schwechat, Austria) equipped with BD FACSDiva software. For analyzing changes in the cell cycle including the sub- $G_1$  area, the obtained FACS data were evaluated using WinMDI 2.9 software (J. Trotter, The Scripps Research

Institute, La Jolla, USA). The cell events were displayed against the red fluorescence of propidium iodide in a histogram. For dividing the cell population into a sub-G<sub>1</sub>, G<sub>0</sub>/G<sub>1</sub>, S- and G<sub>2</sub>/M-phase, markers were placed and the percentage of cells in each state was illustrated.

Apoptotic cells show weaker DNA stainability due to chromatin condensation and DNA fragmentation. Therefore, events exhibiting a lower fluorescence than the G<sub>0</sub>/G<sub>1</sub> peak were considered as apoptotic cells (sub-G<sub>1</sub> peak). Events showing no or very low fluorescence values (below the sub-G<sub>1</sub> phase) consist of debris and fragmented cells and were excluded from evaluation.

### **2.9. Data processing**

Mean values from microplate replicates were corrected for blank values. Unless indicated otherwise, data points represent mean values  $\pm$  S.D. of at least three independent experiments. Statistical analysis was performed by the Student's t-test, with  $p < 0.05$  as criterion of significance.

## **3. Results and discussion**

### **3.1 Polymer synthesis and conjugation with hypericin**

Two synthetic approaches to prepare macromolecular conjugates with hypericin were carried out. In the first approach, hypericin was non-covalently loaded to polyphosphazene polymers functionalized with N-ethylpyrrolidone (Figure 1). The polymers were prepared from polydichlorophosphazene, prepared with narrow molecular weight distributions by living cationic polymerization<sup>32</sup> and macrosubstitution with a large excess of 1-(2-hydroxyethyl)-2-pyrrolidone<sup>36</sup>. After purification, the inorganic-organic hybrid polymers were loaded with hypericin to give HypPYRP (Figure 1). As a comparison, conjugates were also prepared with the non- hydrolytically degradable, PVP to give HypPVP<sup>20</sup>.

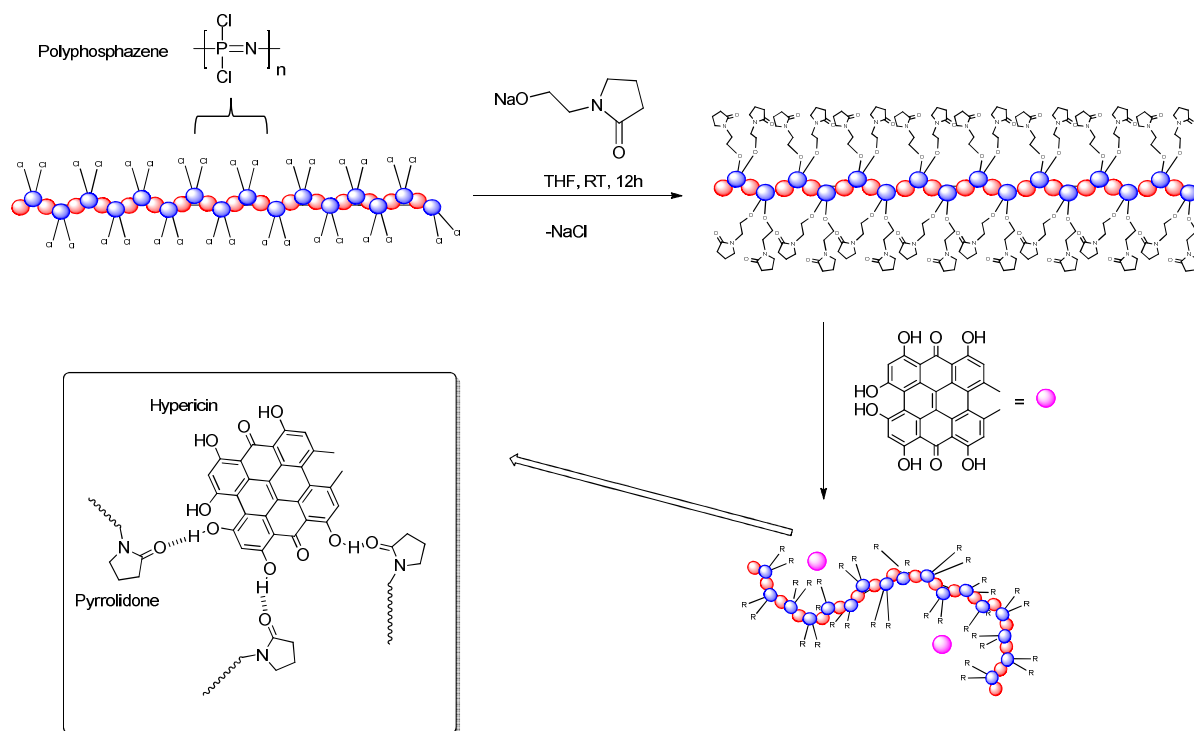


**Figure 1.** Preparation of hypericin conjugates (HypPYRP). Hypericin is presumed to be non-covalently bound to the polyphosphazene carrier via N-ethylpyrrolidone functional groups (see insert), thus enhancing its aqueous solubility.

Although non-covalent binding represents a simple and effective route for the solubilisation enhancement of hydrophobic drugs, covalent binding provides a potentially superior alternative **in terms of structural control of the conjugate**. Thus a second series was also investigated in which the hypericin molecules were covalently bound via their bay-protons (Figure 2). It was recently shown that these protons could be selectively deprotonated to allow covalent attachment to the polydichlorophosphazene backbone<sup>37</sup>. Co-substitution of the polymer carrier with aqueous solubilizing polyalkylene oxide chains (Jeffamine, JFM) gave highly soluble, covalent conjugates of hypericin with  $M_n$  values of approx. 200 kDa for HypJFMP\_1 and 2 and 100 kDa for HypJFMP\_3.

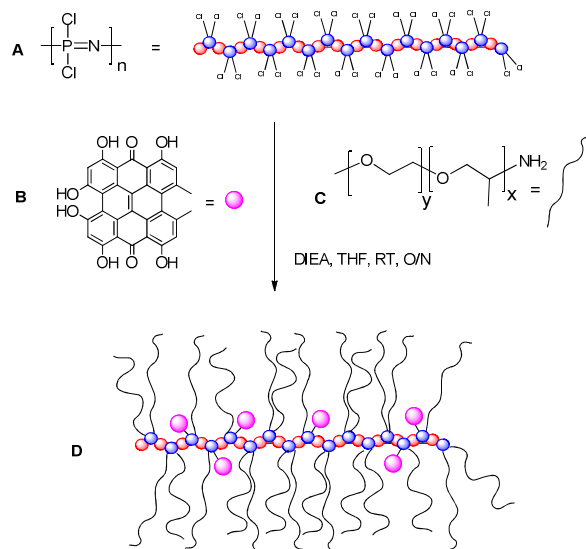


**Figure 2.** Preparation of covalent hypericin conjugates (HypJFMP): Hypericin (B) is covalently bound to the poly(dichloro)phosphazene carrier (A) and co-substituted with aqueous solubilizing Jeffamine (C) (JFM) to give water soluble conjugates (D).

### 3.2 Fluorescence properties of the conjugates

Before application on the cellular level, all conjugates were tested for their solubility and fluorescence properties. All showed excellent solubility in aqueous solutions. Furthermore, the fluorescence properties of all compounds were evaluated. Table 2 presents fluorescence excitation and emission wavelengths, as well as the peak height of the emission peak in relative fluorescence units (r.f.u.) of the new hypericin conjugates. Since the emission peaks are minimally higher than the highest excitation peak at about 600 nm, the latter could not be measured due to overlapping with the peak of Rayleigh scattering. Thus, the emission spectra were recorded using the second highest excitation peak. Fluorescence measurements of the conjugates were carried out with dilutions of 5  $\mu$ M hypericin in aqua bidest, but hypericin was measured in DMSO due its poor solubility in aqueous media and thus the slight red-shift of pristine hypericin compared to the conjugates is likely due to solvent effects. The novel PS conjugates exhibit excitation peaks in the regions of 554 to 557 nm and 596 and 600 nm, with emission peaks around 600 nm. According to the literature, absorbance peaks of hypericin are at 547 nm and 591 nm and emission peaks are located around 600 nm and in the region of 650 to 660 nm<sup>38</sup>. Therefore, the novel formulations show virtually no difference in the excitation and emission wavelength compared to pristine hypericin. Although the activation wavelengths of the photosensitizers does not allow for deep tissue penetration, they have potential use for the treatment of flat tumors such as skin lesions or for diagnostic applications – as it is the case with all known hypericin formulations.

**Table 2.** Fluorescence excitation peaks of hypericin in DMSO and aqueous solutions of its conjugates, the corresponding emission peaks and their height in relative fluorescence units (r.f.u.)

PS ± polymer	$\lambda_{Ex}$ [nm]	$\lambda_{Ex}$ [nm]	$\lambda_{Ex}$ [nm]	$\lambda_{Em}$ [nm]	Peak <sub>Em</sub> height [r.f.u.]
HypPYRP	-	554	596	601	11
HypPVP	480	554	597	601	283
HypJFMP_1	462	557	598	602	140
HypJFMP_2	464	555	600	602	29
HypJFMP_3	462	554	596	602	15
pristine hypericin (in DMSO)*	487	558	602	606	4 200

\*pristine hypericin from Planta Natural Products (Vienna, Austria). This was measured in DMSO as pristine hypericin is insoluble in aqueous media

### 3.3 Dark cytotoxicity of the compounds

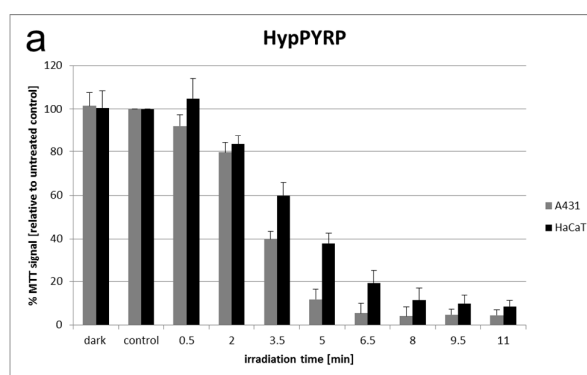
In order to examine, whether the novel PS compounds show effects on cells without irradiation (dark effects), changes in proliferation and cytotoxic reactions with increasing PS concentrations were measured for hypericin concentrations from 1  $\mu$ M up to 80  $\mu$ M. Cell proliferation and cell death was evaluated by measuring cell metabolic activity using an MTT assay and the results on cell viability under dark conditions are shown in the supporting information (Figures ESI 1 – 3). The non-covalently bound hypericin conjugates HypPYRP and HypPVP (Figures ESI 1 and 2) were found to be non-toxic in the dark. However, notable is the cytostatic effect of pristine PYRP and pristine PVP in concentrations corresponding to 1  $\mu$ M of the compound in both cell lines. For the conjugated polymers, the effect is, however, only statistically significant for PYRP and only on A431, not on HaCaT cells. When PVP is conjugated to hypericin a cytostatic effect at 1  $\mu$ M is not visible. The obvious damage by the polymers seems to be repaired at higher doses by the onset of specific repair mechanisms and also by the presence of hypericin; the latter seems to compensate the damage by supporting proliferation. The polymer PYRP is cytostatic above 70  $\mu$ M (A431 cells) or 50  $\mu$ M (HaCaT cells), respectively. The photosensitizer-conjugate HypPVP (Figure ESI 2) causes a moderate proliferative effect up to a concentration of 50  $\mu$ M in A431 cells. For concentrations above 50  $\mu$ M the MTT signal remains at the control level. In the non-malignant HaCaT cells the proliferative effect can be found statistically significant for concentrations between 10  $\mu$ M and 30  $\mu$ M.

Incubation of A431 and HaCaT cells with the covalently bound PSs shows different results for the three conjugates (Figure ESI 3). While HypJFMP\_1 (Figure ESI 3a), with the lowest loading of hypericin, has almost no effect on the viability of both cell lines, similar to the pristine polymer, HypJFMP\_2 (Figure ESI 3b) induces a proliferative response at higher hypericin concentrations, from 20  $\mu$ M (A431 cells) or 50  $\mu$ M (HaCaT cells), respectively. HypJFMP\_3 (Figure ESI 3c), with the highest loading of hypericin is the only photosensitizer, which exhibits a rather strong dark cytotoxicity on both cell lines *per se*, beginning at 50  $\mu$ M. One reason for the different results of the JFMP conjugates might be the varying ratios between polymer and hypericin. While HypJFMP\_1 contains a rather small amount of

hypericin (0.7%), HypJFMP\_2 contains more than twice as much (1.6%), which in turn is duplicated in HypJFMP\_3 (3.4%), i.e the proportion of hypericin in the molecule increases significantly from JFMP\_1 to \_3. The proliferative response to HypJFMP\_2 could be attributed to its hypericin fraction, since the pristine polymer rather has the tendency to slow proliferation down. The effect might be caused by the subdued light conditions in which dark cytotoxicity experiments were carried out; at the relatively high hypericin concentrations used even small amounts of light are sufficient to produce reactive oxygen species, which trigger sublethal damage signaling in the cells. Cells are able to repair the damage and subsequently perform mitosis, which might account for the increase in cell numbers. HypJFMP\_3 is smaller than the other two HypJFMP conjugates, it contains the highest amount of hypericin molecules and is therefore comparably lipophilic. This feature may be responsible for its cytotoxic effect on both cell lines. HypJFMP\_1 in contrast, induces only little proliferative response in A431 cells and no cytostatic effect. This is consistent with the comparably low phototoxicity and fluorescence values of HypJFMP\_1 (see later).

In a previous study it could be shown that pure hypericin causes an increase in proliferation at low doses in both A431 and HaCaT cells, while higher concentrations lead to cytostatic effects and cytotoxicity in A431 cells, but not in HaCaT cells<sup>39</sup>. Similar to the results presented here, Vandenbergaeerde *et al.*<sup>40</sup> have shown that hypericin-mediated dark cytotoxicity does not occur up to 25  $\mu\text{M}$  hypericin and incubation periods of 24 hours in A431 cells. Cytostatic effects of hypericin without irradiation<sup>41</sup> are explained by inhibition of several key enzymes (growth-factor regulated protein kinases) involved in cell proliferation signaling pathways *in vitro*<sup>42</sup>. Furthermore, small amounts of ROS produced during handling are known to affect cellular signaling pathways which support proliferation<sup>13</sup>. When the amount of ROS exceeds a certain threshold, proliferation is reduced or stopped and apoptosis is induced<sup>13</sup>. Additionally, due to its low redox potential, hypericin can function as an electron acceptor from physiological electron transfer reactions, as well as an electron donor to generate reactive oxygen species. Therefore, hypericin can act under dark conditions as both an oxidizing and reducing agent<sup>43</sup>.

### 3.4 Phototoxicity of the compounds



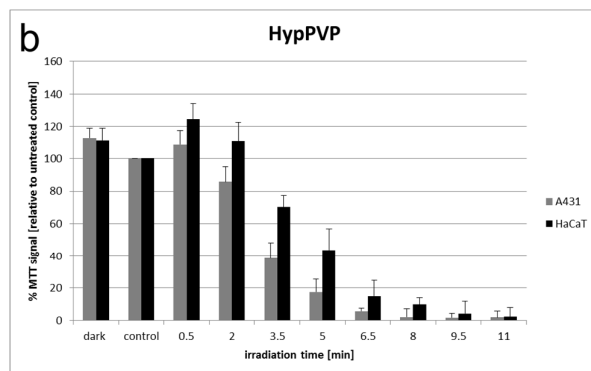


**Figure 3.** Light-dependent cytotoxicity of the non-covalently bound photosensitizers (a) HypPYRP (5  $\mu$ M) and (b) HypPVP (5  $\mu$ M) in A431 and HaCaT cells. Cell survival in % was related to the untreated control  $C_0$ . Irradiation parameters:  $\lambda_{\max} = 610 \pm 10$  nm; power density = 1.8 mW/cm<sup>2</sup>.

The ability of hypericin to trigger cell death in PDT with red-light irradiation has been well documented for numerous cell lines (see e.g. the review of Karioti et al.<sup>12</sup>) and hence it was investigated in this study whether the novel hypericin-polymer conjugates possess comparable efficiencies *in vitro*.

In order to achieve similar dose-effect curves for each photosensitizer-conjugate the photosensitizing dose (sensitizer x irradiation) was adapted by various irradiation times and therefore different fluences. A431 cells incubated with 5  $\mu$ M (relative hypericin concentration) HypPYRP (Figure 3a) shows a rapid loss of viability with increasing irradiation times, compared to the untreated control. Under the present conditions, an irradiation time of 6.5 min (corresponding to a fluence of 0.70 J/cm<sup>2</sup>) eradicates approximately 95 % of all cancer cells. Notably, even irradiation times of 8 min ( $\pm$  0.86 J/cm<sup>2</sup>) and longer do not erase the remaining cell population. At irradiation times of 0.5 min ( $\pm$  0.05 J/cm<sup>2</sup>), HaCaT cells show an increase in viability for about 5 %. Between 0.5 and 6.5 min irradiation time, reduction of cell viability is nearly linear. A fluence of 1.03 J/cm<sup>2</sup> (equals 9.5 min of irradiation) eradicates the maximum of 90 % of all cancer cells. As a comparison the known photosensitizer conjugate HypPVP was also tested (Figure 3b): after incubation of A431 cells, the MTT signal decreases continuously with rising irradiation times. At 0.5 min, A431 cells show an increase of proliferation of about 12 %. From 0.5 to 6.5 min irradiation, cell survival declines in a near linear manner. After 8 min of irradiation > 98 % of all cancer cells are eradicated. HaCaT cells showed similar behaviour, with shorter irradiation times of 0.5 to 2 min ( $\pm$  0.05 to 0.22 J/cm<sup>2</sup>) leading to an increase of proliferation for almost 30 %, with longer irradiation times reducing the amount of living cells up to approximately 1 % at 11 min. This initial proliferative stimulation was observed for both conjugates tested and could be due to the effect described previously for the dark cytotoxicity experiments that low irradiation doses produce low ROS levels and thus limited damage which the cells can repair with adaption processes triggering proliferative pathways.

Furthermore, neither of the pristine polymers PYRP or PVP showed any effect on cell survival (data not shown) with the MTT signal remaining at the level of the untreated control under equivalent conditions.

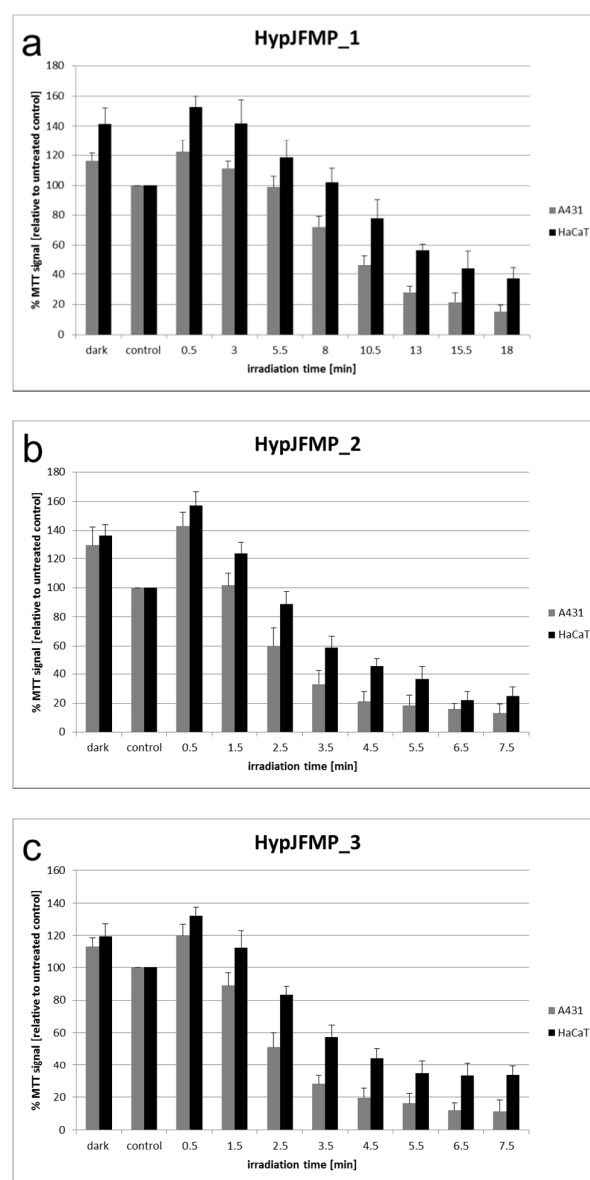


**Figure 4.** Light-dependent cytotoxicity of the covalently bound photosensitizers (a) HypJFMP\_1, (b) HypJFMP\_2 and (c) HypJFMP\_3, (each 5  $\mu\text{M}$ ) in A431 and HaCaT cells. Cell survival in % was related to the untreated control  $C_0$ . Irradiation parameters:  $\lambda_{\text{max}} = 610 \pm 10 \text{ nm}$ ; power density = 1.8  $\text{mW}/\text{cm}^2$ .

A431 cells incubated with 5  $\mu\text{M}$  (relative hypericin concentration) of HypJFMP\_1 (Fig. 4a) show a decrease in cellular survival, a signal of less than 20 % being reached after 18 min of irradiation ( $\approx 1.94 \text{ J}/\text{cm}^2$ ). For irradiation times of 0.5 to 3 min, A431 cells present an increase in viability of about 22 %. Incubation of the HaCaT cells with the same compound has a similar progression. Shorter irradiation times of 0.5 to 8 min ( $\approx 0.05$  to  $0.86 \text{ J}/\text{cm}^2$ ) lead to an increase in viability (almost 55 %), while irradiation times longer than 8 min reduce the amount of viable cells to less than 40 %. In contrast, when A431 cells are treated with HypJFMP\_2 at the same hypericin concentration (Figure 4b), their survival is decreased to less than 15 % after just 7.5 min of irradiation ( $\approx 0.81 \text{ J}/\text{cm}^2$ ). For irradiation times of 0.5 min, cells present an increase of viability of about 42 %. Generally, an irradiation time of 5.5 min (which corresponds to  $0.59 \text{ J}/\text{cm}^2$ ) is sufficient to eradicate nearly 85 % of all cancer cells.

HaCaT cells show similar behaviour, with irradiation times of 0.5 to 1.5 min ( $\pm 0.05$  to  $0.16 \text{ J/cm}^2$ ) presenting an increase in viability of almost 60 %, while for longer irradiation times, survival drops to approximately 25 % at 6.5 min. Following an irradiation time of 0.5 min for HypJFMP\_3 (5  $\mu\text{M}$  hypericin) (Figure 4c), an increase of viability of about 22 % can be measured in A431 cells. Between 0.5 and 4.5 min ( $\pm 0.05$  to  $0.49 \text{ J/cm}^2$ ) irradiation, reduction of cell viability is nearly linear. An irradiation with  $0.60 \text{ J/cm}^2$  (equals 5.5 min of irradiation) is sufficient to eradicate > 85 % of all cancer cells. Incubation of HaCaT cells with the same compound shows a similar progression in cell death. Irradiation times of 0.5 to 1.5 min present an increase of viability of about 30 %, while for higher fluences, survival decreases to approximately 35 % at 6.5 min irradiation time without further progression. This effect was observed for all conjugates tested, that is when increasing the fluence, maximum lethality between 1 - 30 % for both cell lines is reached, which cannot be further decreased. In control studies, none of the pristine JFMPs tested showed any phototoxic effects (data not shown).

**Table 3.** Photosensitizing efficiency in A431 and HaCaT cells.  $\text{LD}_{50}$  values in both cell lines are shown as irradiation time in min.

Photosensitizer	$\text{LD}_{50, \text{PDT}}$ [min.]	$\text{LD}_{50, \text{PDT}}$ [min.]
	A431	HaCaT
HypPYRP	3.09	4.15
HypPVP	3.25	4.63
HypJFMP_1	10.29	14.37
HypJFMP_2	2.92	4.63
HypJFMP_3	2.67	4.05

The photosensitizing efficiency of the conjugates is summarized in table 3. Similar  $\text{LD}_{50}$  times are attained for the non-covalent polymers HypPVP and HypPYRP. The covalently bound HypJFMP\_2 and HypJFMP\_3 also have  $\text{LD}_{50}$  in a similar region, although. HypJFMP\_1 requires a more than three times higher fluence than the two other covalently bound polymers for  $\text{LD}_{50}$  and can therefore be regarded as less effective: This is presumably due to the sterical constriction of hypericin uptake caused by the relatively high polymer to hypericin ratio (99.3 % wt), an observation consistent with the uptake kinetics (see later).

A431 cells show a decline in viability at lower fluences than HaCaT cells, resulting in shorter irradiation times at  $\text{LD}_{50}$ . That is, A431 cells exhibit a 1.3 to 1.6-fold higher sensitivity to PDT with the hypericin-conjugates than HaCaT cells. Tumor selectivity of hypericin on the in-vitro level has neither been observed before in our laboratory nor been reported in literature. The origin of this tumor selectivity was proposed to be the cell-uptake kinetics, which were duly tested.

### 3.5 Uptake kinetics

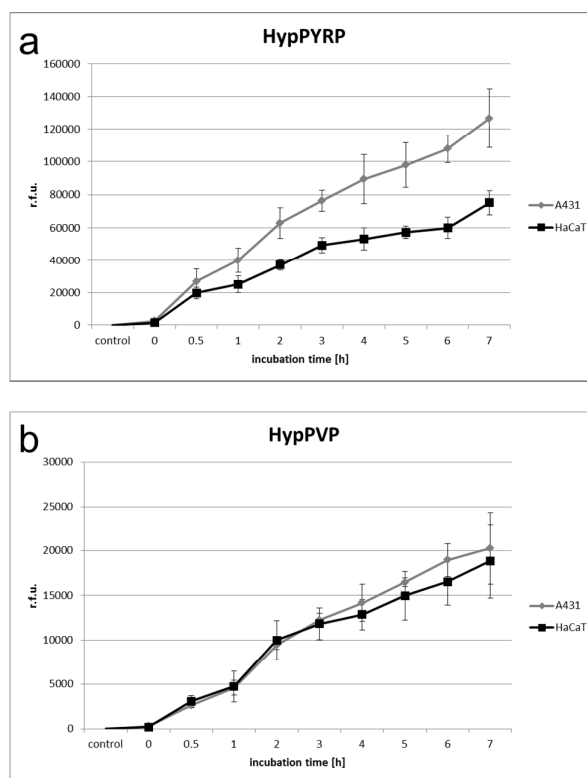


**Figure 5.** Uptake kinetics of hypericin non-covalently bound in (a) HypPYRP and (b) HypPVP, both in a concentration of 5  $\mu\text{M}$  in A431 and HaCaT cells. Hypericin fluorescence was plotted as fluorescence intensity per protein in relative fluorescent units (r.f.u.).

Uptake kinetic studies of the photosensitizers were carried out in A431 and HaCaT cells over a time period of 7 hours with a hypericin concentration of 5  $\mu\text{M}$ . As expected, hypericin fluorescence indicating the amount of photosensitizer incorporated into the cells increases with incubation time (Figure 5). A431 cells incubated with HypPYRP (5  $\mu\text{M}$  hypericin) (Figure 5 a) reach a hypericin fluorescence level of approximately 125 000 r.f.u after 7 hours of incubation. In HaCaT cells, the amount of incorporated hypericin after 7 hours is 1.7-fold lower than in A431 cells with about 75 000 r.f.u., but the kinetics is also nearly linear up to the longest incubation time. Similar results were obtained for the uptake of hypericin in the HypPVP series in A431 and HaCaT cells, (Figure 5 b), with the course of both curves being almost linear within 7 hours of incubation, although here the minimally higher uptake to A431 cells observed is not significant. It is remarkable that in both cell lines, hypericin in HypPYRP has the highest apparent uptake (Table 4) despite having a similar resulting phototoxicity ( $\text{LD}_{50}$ ) as HypPVP. Hypericin in HypPYRP shows higher final fluorescence values of a factor of 4 (HaCaT cells) to 6 (A431 cells) over hypericin in HypPVP. Thus phototoxicity and fluorescence values do not correlate, suggesting that fluorescence levels of the compounds within the cells not only reflect the amount of accumulated PS, but also physico-chemical changes such as quenching effects.

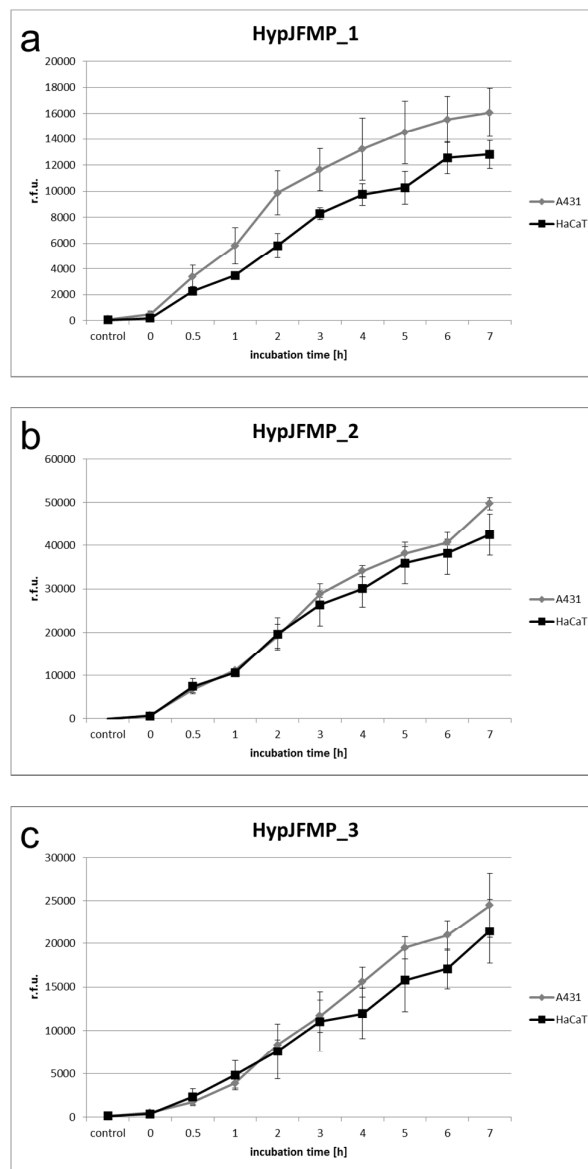


**Figure 6.** Uptake kinetics of hypericin covalently bound in (a) HypJFMP\_1, (b) HypJFMP\_2 and (c) HypJFMP\_3, all in a concentration of 5  $\mu\text{M}$  in A431 and HaCaT cells. Hypericin fluorescence was plotted as fluorescence intensity per protein in relative fluorescent units (r.f.u.).

Figure 6 shows the uptake kinetics for hypericin in the covalent HypJFMP series. A431 cells incubated with HypJFMP\_1 (5  $\mu\text{M}$  hypericin) reach a hypericin fluorescence of approximately 16 000 r.f.u. after 7 hours of incubation (Fig. 6 a). In comparison the amount of incorporated hypericin in HypJFMP\_1 after 7 hours is 1.3-fold lower in HaCaT cells than in A431 cells. For both cell lines, a nearly linear uptake can be observed with a moderate tendency to form a plateau. A comparison of the accumulation of hypericin in HypJFMP\_2 in A431 and HaCaT cell lines shows an almost identical, linear course (Figure 6 b); however the fluorescence values are slightly higher for A431 cells (1.2-fold higher) from 3 hours on. Incubation of A431 cells with HypJFMP\_3 (5  $\mu\text{M}$  hypericin concentration) causes an uptake maximum of

approximately 24 000 r.f.u. after 7 hours of incubation (Figure 6 c). The uptake of hypericin in HypJFMP\_3 after seven hours in HaCaT cells is 1.1-fold lower than in A431 cells. In both cell lines the accumulation kinetics of the compound are nearly linear.

Hypericin in HypJFMP\_1 exhibits the lowest fluorescence values, which could explain the previous observation that HypJFMP\_1 proved to be the least effective compound in the phototoxicity studies. Hypericin in HypJFMP\_2 shows the highest fluorescence values of the covalently bound conjugates in both cell lines, correlating with a high phototoxicity. However, despite exhibiting a phototoxicity similar to that of HypJFMP\_2, hypericin in HypJFMP\_3 has approximately 50% lower fluorescence values for both cell lines. It is likely that the percentage of hypericin in the conjugates is reflected in the observed intracellular fluorescence values: 0.7% hypericin in HypJFMP\_1 entails a relatively high ratio of polymer to hypericin, and thus a dilution of the PS. Whereas it is possible that hypericin in HypJFMP\_3 is too densely packed, resulting in phototoxicity not exceeding that of HypJFMP\_2 and in a lower fluorescence level, probably due to self-quenching or aggregation effects.

As a consequence of their chemically diverse characteristics and the observed quenching effects, a quantitative comparison of the actual uptake kinetics between the HypJFMP series, and moreover between all hypericin conjugates, is unfortunately not possible.

**Table 4.** Accumulation of the non-covalently and covalently bound photosensitizers after seven hours of incubation in A431 and HaCaT cells. Hypericin fluorescence is shown as fluorescence intensity per protein in relative fluorescent units (r.f.u.)

Photosensitizer	r.f.u.	r.f.u.
	A431	HaCaT
HypPYRP	126 674 ( $\pm$ 17 975)	75 143 ( $\pm$ 7 337)
HypPVP	20 272 ( $\pm$ 4 026)	18 848 ( $\pm$ 4 138)
HypJFMP_1	16 070 ( $\pm$ 1 849)	12 815 ( $\pm$ 1 095)
HypJFMP_2	49 727 ( $\pm$ 1 429)	42 539 ( $\pm$ 4 829)
HypJFMP_3	24 450 ( $\pm$ 3 730)	21 450 ( $\pm$ 3 722)

Table 4 summarizes the PS accumulation after 7 hours incubation. It is apparent that higher fluorescence values of all hypericin conjugates are observed in A431 than in HaCaT cells. It seems that all novel compounds exhibit at least some tumor selectivity (1.1 to 1.6-fold within 7 h) in PS fluorescence, which can be correlated to PS accumulation when fluorescence quenching effects are neglected. This may explain the enhanced tumor-selectivity observed in A431 cells (see previous section). However, hypericin in HypPYRP is the only novel photosensitizer conjugate, where higher uptake (1.7 fold) in A431 cells compared to HaCaT cells could be classified as significant.

In the literature, two uptake mechanisms are described for pristine hypericin. Cellular uptake may occur *via* passive processes, such as diffusion, or by membrane-associated translocation processes, such as pinocytosis and interactions between hypericin and serum constituents (e.g. BSA and LDL)<sup>1,8,44</sup>. For PVP-hypericin its exact uptake mechanism is still unknown<sup>45</sup>. However, pristine PVP, as with most macromolecules, is known to be taken up by cells and accumulated in lysosomes<sup>24,25,46</sup>.

### 3.6 Intracellular localization

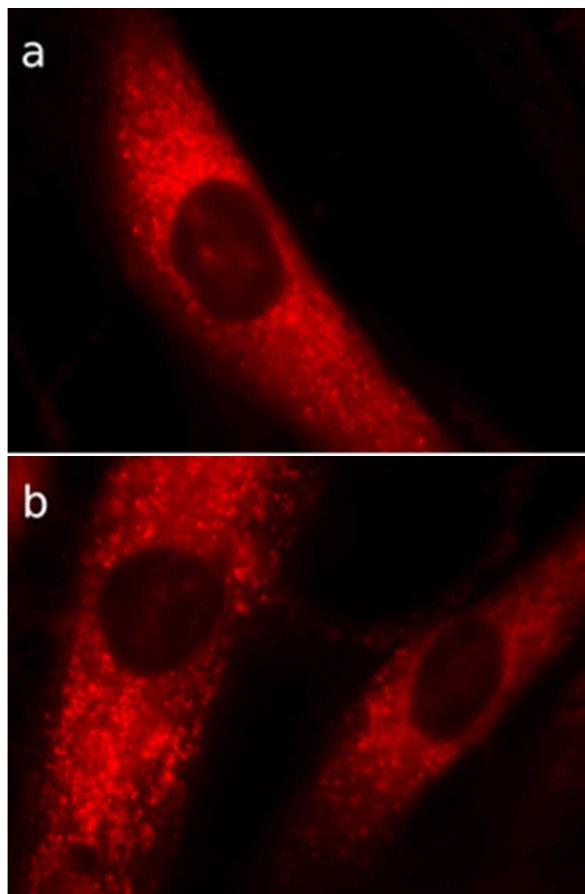
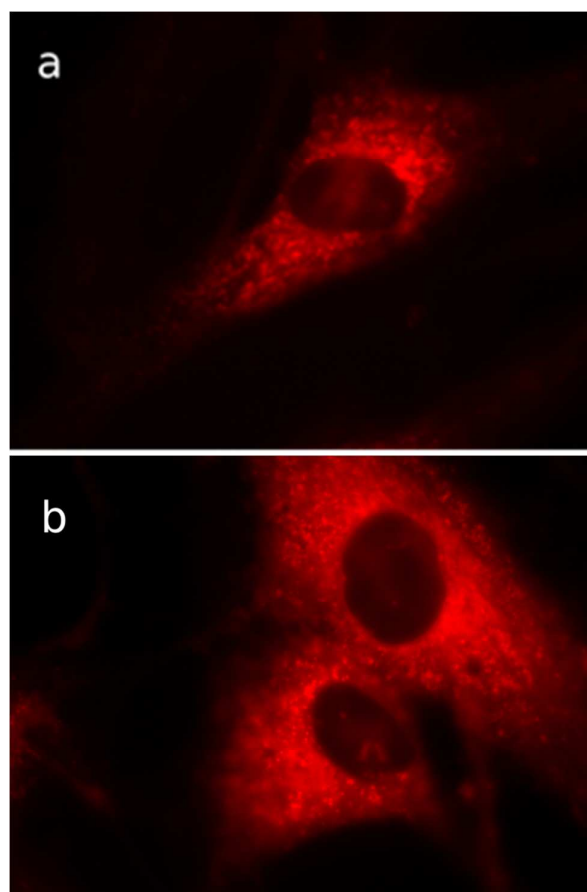


**Figure 7.** Localization of 5  $\mu\text{M}$  hypericin non-covalently bound in HypPYRP (a) and HypPVP (b) in primary human dermal fibroblasts after 3 hours of incubation. 1000x magnification; oil-immersion (filter:  $\lambda_{\text{Ex}} = 480 - 500$  and  $\lambda_{\text{Em}} > 570$  nm).

The intracellular localization of a photosensitizer is a critical feature for PDT efficiency. Since ROS have only a short half-life, they act close to their site of generation. Consequently, the type of photodamage that occurs in cells after irradiation is influenced by the intracellular localization of the photosensitizer<sup>47</sup>. The intracellular distribution of a photosensitizer usually depends on its chemical and physical features, including net ionic charge, hydrophobicity, and molecular size and symmetry. As hypericin is a hydrophobic molecule, it can easily cross the plasma membrane (by whatever mechanism) and bind to the intracellular lipid matrix of membranes<sup>38,47</sup>.

In this study, we recorded the localization of all novel hypericin formulations in dermal fibroblasts, as shown in Figures 7 and 8, since this cell line is better suited for fluorescence

microscopy than A431 or HaCaT cells due to its planar morphology and its relatively large cytoplasmic region. After three hours of incubation, hypericin from all conjugates was observed to localize in the Golgi apparatus and in the endoplasmic reticulum (ER), excluding the nucleus (Figures 7 and 8). Additionally, strong hypericin fluorescence can be observed in lysosomes. Lysosomes, although not exclusively, are a critical intracellular target in PDT. They are responsible for degrading waste materials and cellular debris. Kessel *et al.*<sup>48</sup> showed that photosensitizers, localizing in the lysosomes cause the release of cathepsins from these organelles into the cytoplasm. Once in the cytosol, cathepsins can either cleave Bid, leading to apoptosis or induce autophagy<sup>49</sup>. The localization of hypericin in lysosomes, as found in the present study also suggests that photodamage in these organelles contributes to cell death. Hypericin is excluded from the nucleus indicating the absence of genotoxic effects. Even after longer incubation times (up to nine hours) no re-localization was observed (data not shown). Generally it can be concluded that the localization of hypericin from the different conjugates in these organelles also leads to ROS formation upon irradiation *ibidem*, which in turn triggers apoptosis or autophagy or leads to necrosis at higher PDT doses.



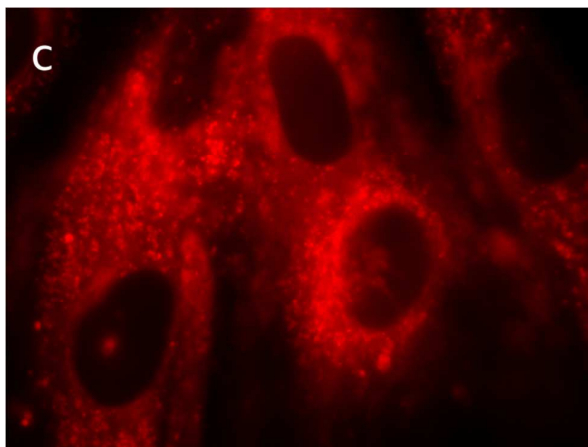


**Figure 8.** Localization of 5  $\mu\text{M}$  hypericin covalently bound in (a) HypJFMP\_1, (b) HypJFMP\_2 and (c) HypJFMP\_3 in primary dermal fibroblasts after 3 hours of incubation. 1000x magnification; oil-immersion (filter:  $\lambda_{\text{Ex}}$  = 480 - 500 nm and  $\lambda_{\text{Em}}$  > 570 nm).

Pristine hypericin has been reported to accumulate in different cell lines in ER, Golgi apparatus and/or lysosomes, but less in mitochondria<sup>50</sup>. Hyp-PDT is often accompanied by the release of calcium from the ER and an increase in intracellular  $\text{Ca}^{2+}$  levels, which can contribute to apoptosis by activating the  $\text{Ca}^{2+}$ -calpain pathway, triggering mitochondrial pore opening<sup>51</sup>. It was suggested that this shift in cytoplasmic  $\text{Ca}^{2+}$  levels results from photodamage set to  $\text{Ca}^{2+}$ -binding proteins in the ER<sup>50</sup>. The Golgi complex is in a close spatial as well as dynamic functional relationship with the ER; it modifies proteins delivered from the ER and releases them into the extracellular medium. Similar to the ER stress-response-pathway, the Golgi apparatus may also initiate signaling pathways to deal with stress and trigger apoptosis<sup>52</sup>. Thus photodamage by hypericin located in the Golgi complex, as found by Ritz et al<sup>53</sup> may also be involved in apoptosis induction.

### 3.6 Cell cycle analysis and apoptosis detection by the sub- $G_1$ assay of the compounds

Post PDT dose-dependent cell cycle alterations and DNA fragmentation, indicating apoptosis induction, were evaluated for all compounds via DNA staining with propidium iodide by flow cytometry. The majority of untreated A431 and HaCaT cells show a normal diploidic DNA content, which is consistent with a large fraction of cells in the  $G_0/G_1$  phase (approximately 50 %). Almost 50 % of the events are allotted to the smaller fractions of the S-phase (doubling the DNA content), of the  $G_2/M$  phase (doubled DNA content), and of the sub- $G_1$ -phase (Figure ESI 4-6). For PDT treatment, 5  $\mu\text{M}$  of the compounds and three different fluences, represented by different irradiation times, were chosen based on the phototoxicity experiments: 0.5 min for all compounds (shortest irradiation time, equals 0.05  $\text{J}/\text{cm}^2$ ); further 3.5 min for HypPYRP and HypPVP, 10.5 min for HypJFMP\_1, and 2.5 min for HypJFMP\_2 and HypJFMP\_3 (approximately  $\text{LD}_{50}$ ); and finally 11 min for HypPYRP and HypPVP, 18 min for HypJFMP\_1, and 7.5 min for HypJFMP\_2 and HypJFMP\_3 (longest irradiation times).

#### 3.6.1 Sub- $G_1$ -phase

In the untreated and dark control samples of both cell lines, the sub- $G_1$  fraction remains under 5 % (Figure ESI 4-6). Also, after incubation of both cell lines with the pristine polymers PYRP, PVP and JFMP, the sub- $G_1$  fraction remained under 5% irrespective whether irradiated or not (data not shown).

Irradiation of HypPYRP for 0.5 min causes no significant change in the sub-G<sub>1</sub> fraction, but longer irradiation times of 3.5 and 11 min lead to an accumulation of 45 % of A431 and 35 % of HaCaT cells in the sub-G<sub>1</sub> fraction (Figure ESI 4). The apoptotic events of HaCaT cells treated with HypPYRP-PDT are moderately reduced. While both cell lines increase their apoptosis induction from 3.5 to 11 min irradiation when incubated with HypPVP, they reach their maximum apoptosis rate already at 3.5 min when incubated with HypPYRP; thus both cell lines are more sensitive to PDT with HypPYRP (Figure 4). After HypPVP-PDT, almost half of the measured cells undergo apoptosis, as demonstrated by the significant accumulation of the cells in the sub-G<sub>1</sub> fraction (approximately 46 % for both cell lines) (Table 5, Figure ESI 5).

**Table 5:** Percentage of cells with DNA fragmentation (sub-G<sub>1</sub> fraction) after PDT with the different Hyp-conjugates at three irradiation times: T1: shortest irradiation time; T2: approx. 50 % dead cells; T3: longest irradiation time.

<b>A 431: % cells in sub-G<sub>1</sub></b>			
<b>conjugates</b>	<b>T1</b>	<b>T2</b>	<b>T3</b>
HypPYRP	6.08 (± 2.31)	43.67 (± 7.67)	44.68 (± 7.66)
HypPVP	4.16 (± 0.38)	32.51 (± 9.12)	46.49 (± 9.18)
HypJFMP_1	4.36 (± 1.89)	51.76 (± 11.62)	56.74 (± 9.92)
HypJFMP_2	5.17 (± 1.92)	36.22 (± 8.3)	37.1 (± 1.99)
HypJFMP_3	3.31 (± 1.68)	16.97 (± 4.62)	43.83 (± 0.53)

<b>HaCaT: % cells in sub-G<sub>1</sub></b>			
<b>conjugates</b>	<b>T1</b>	<b>T2</b>	<b>T3</b>
HypPYRP	2.58 (± 0.14)	32.65 (± 4.83)	34.44 (± 6.03)
HypPVP	3.55 (± 0.78)	25.65 (± 5.99)	46.31 (± 4.24)
HypJFMP_1	2.78 (± 0.73)	41.25 (± 5.23)	43.88 (± 2.78)
HypJFMP_2	3.39 (± 1.01)	13.72 (± 2.88)	27.04 (± 6.25)
HypJFMP_3	2.05 (± 0.23)	6.58 (± 1.46)	30.5 (± 4.66)

The covalently bound JFMP photosensitizers exhibit similar results, although with different irradiation times: A431 cells show the highest fraction of cells with fragmented DNA (–up to 55 %) while in HaCaT cells this portion is significantly smaller (up to 45 %) with all three conjugates.

When A431 cells were incubated with HypJFMP\_1 and irradiated, the percentage of cells in the sub-G<sub>1</sub> fraction increased significantly (to approximately 55 %). The same effect can be

observed in the HaCaT cell line; indeed the percentage of cells in the sub-G<sub>1</sub> fraction is lower (approximately 45 %) (Figure ESI 6a). A431 cells incubated with HypJFMP\_2 show a moderately increased accumulation of cells in the sub-G<sub>1</sub> area at 0.5 min, which after 2.5 and 7.5 min (corresponding to 0.27 and 0.81 J/cm<sup>2</sup>) markedly increases (up to approximately 38 %). HaCaT cells also present with the highest fluence (0.81 J/cm<sup>2</sup>) about 28 % increase of the sub-G<sub>1</sub> fraction (Figure ESI 6b).

With increasing irradiation time of HypJFMP\_3 almost half or a third, respectively, of the cells of both cell lines undergo apoptosis, as demonstrated by the significant accumulation of cells in the sub-G<sub>1</sub> fraction at the highest fluence (approximately 44 % for A431 and 30 % for HaCaT cells) (Figure 6c). Comparison of the phototoxicity of all compounds with the apoptotic sub-G<sub>1</sub> fraction, reveals that apoptosis is responsible for cell death to a major extent applying the selected PDT protocols. 38 – 55 % of the A431 cells and 28 – 42 % of the HaCaT cells were found in the apoptotic fraction after irradiation with the respective highest fluence at the time of investigation at 8 h post-irradiation. At 24 h post-irradiation, phototoxicity measurements recorded more than 60% dead cells, which have been killed by both, apoptosis and necrosis. Apoptosis results are in agreement with Berlanda *et al.*<sup>54</sup> who showed that the cell death mode of hypericin in A431 cells is dose-dependent, inducing apoptosis at lower doses, whereas higher fluences favour necrotic cell death. Hypericin causes a light-induced acidification of the cytosol. Therefore, a rapid proton transfer reaction takes place, in the excited state of hypericin, from one hydroxyl group to the adjacent carbonyl moiety<sup>12</sup>. Several reports indicate that an intracellular pH drop of the cytosol is associated with apoptosis. The extent of the pH change varied in the literature, but typically represents a drop of 0.3 - 0.4 pH units. It seems that the decrease in cytosolic pH precedes caspase activation in cells undergoing apoptosis<sup>55</sup>. Additionally, as in the present study, localization of the PS in lysosomes leads to destruction of the latter upon irradiation and release of acid enzymes. Furthermore, apoptosis induction is correlated with the amount of damage induced in the ER and Golgi-complex by ROS<sup>54</sup>. The mode and the amount of conjugation of hypericin with polymers do not seem to play a major role in apoptosis induction, since the effects can be attributed to hypericin.

A reduced apoptosis rate in HaCaT compared to A431 cells after PDT with each compound except HypPVP can be correlated with a generally lower phototoxicity (LD<sub>50</sub> and highest fluence). A reason for the restricted susceptibility of HaCaT cells towards PDT could be that they contain two heterozygous p53 mutations (exons 5 and 8). The tumor suppressor protein p53 is normally crucial for the regulation of the cell cycle, it induces cell cycle arrest and repair after DNA damage and plays an important role in the initiation of apoptosis. Lack of p53 function seems to impede apoptosis induction and with it cell death. Lee *et al.*<sup>56</sup> analyzed in a cell line, overexpressing a dominant negative form of p53, whether Hyp-PDT-induced apoptosis is dependent on the presence of functional p53 proteins. To achieve this they treated osteosarcoma cells and an isogenic cell line having intact p53 with hypericin and light. In contrast to our results, they found that neither hypericin uptake, phototoxicity, cell cycle arrest nor the ability to undergo apoptosis was altered. However, other authors describe contradicting findings indicating delayed activation of caspase-3 following Hyp-PDT due to a lack of functional p53<sup>57</sup>.

### 3.6.2 Cell Cycle

While the sub-G<sub>1</sub> fraction increased with longer irradiation times, the G<sub>0</sub>/G<sub>1</sub>, as well as the G<sub>2</sub>/M fractions, decreased accordingly in all compounds. Corresponding to the reduced

apoptosis rate in HaCaT cells, the decrease of the  $G_0/G_1$  fraction is less pronounced in HaCaT cells; with even an unchanged  $G_0/G_1$  fraction being found for HypPVP, HypJFMP\_2 and \_3. This could indicate cell cycle arrest for damage repair. No major changes with increasing radiation were detected in the S-phase (Figures ESI 4-6). When both cell lines were incubated with all compounds in the dark, no significant differences to the untreated control in all cell cycle phases (Figures ESI 4-6) were observed. Also incubation with the pristine polymers PYRP, PVP and JFMP caused no significant changes in the cell cycle compared to the control sample (data not shown).

Apart from a more or less pronounced reaction of the cells dependent on the applied fluence, the response pattern of the cell cycle to PDT treatments with the various conjugates is similar. Comparative cell-cycle analyses with hypericin as a photosensitizer are rarely reported in the literature. Wang *et al.*<sup>58</sup> showed that HYP-PDT with the human nasopharyngeal carcinoma cell line CNE-2 causes a decrease of cells in the  $G_1$  phase, while the proportions of cells in the S and  $G_2$  phase increased. Hypericin without irradiation caused a small amount of apoptotic cells; however, the percentage of apoptotic cells after hypericin treatment and irradiation was markedly higher<sup>55</sup>. Similarly to the present results, Sačková *et al.*<sup>55</sup> observed that hypericin causes an accumulation of U937 cells (human myeloid leukemia cell line) in the S phase accompanied by a decline in cell number in the  $G_0/G_1$  phase. At the same time, the percentage of cells in the sub- $G_1$  phase was significantly increased. On the other hand, HT-29 cells (human colon adenocarcinoma cell line) were arrested in the  $G_2/M$  phase of the cell cycle, when treated with Hyp-PDT<sup>55</sup>. Thus, the influence of Hyp-PDT on cell cycle phases seems to differ according to the cell line.

#### 4. Conclusions

In the present study it could be shown that (i) the novel photosensitizer conjugates exhibit excitation and emission wavelengths comparable to that of pristine hypericin, (ii) hypericin conjugated with polyphosphazenes has no toxic effects without irradiation; with the exception of the highest hypericin loaded polymer HypJFMP\_3, which shows a ratio-dependent dark toxicity above 50  $\mu\text{M}$  on both cell lines, (iii) the pristine polymers (PYRP, PVP or JFMP) are not toxic in both cell lines, however some cytostatic effects especially of PYRP can be observed at certain concentrations, (iv) A431 cells show a decrease in viability at lower light fluences than HaCaT cells exhibiting a 1.3 to 1.6-fold higher sensitivity after irradiation with light doses at an  $\text{LD}_{50}$ , (v) hypericin from these novel hydrolytically degradable conjugates accumulates faster and to a higher extent in A431 than in HaCaT cells, when fluorescence quenching effects are neglected, an effect not observed in previous studies with PVP-hypericin, (vi) the photosensitizer conjugates are efficient inducers of apoptosis, as can be shown via nuclear fragmentation detection and (vii) all sensitizers localize in the same subcellular structures namely the endoplasmic reticulum, Golgi complex and lysosomes.

During the recent expansion in the use of polymers for nanomedicine, it has become apparent that the use of non-degrading, biopersistent high MW polymers such as PVP and PEG can lead to long-term deleterious effects, in particular for intravenous applications and where high doses are required. Thus the search for viable, hydrolytically degradable alternatives is paramount. The novel polymers PYRP and JFMP prove to be promising hydrolytically degradable carriers for the delivery of hypericin for PDT, significantly enhancing solubility of the free drug without compromising the photoactivity. The phototoxic results

obtained for the covalently bound photosensitizers show a dependency on the polymer: photosensitizer ratios, which must be taken into account when evaluating the applicability of hypericin-conjugates in PDT, with small sterical modifications altering to a major extent its dark- and phototoxicity, cytostatic effects and cellular accumulation. The non-covalent formulation of hypericin with PYRP would be an optimal hydrolytically degradable alternative to the known hypericin-PVP conjugate, proving to be equally effective in the destruction of tumor cells as HypPVP and showing a 4-6 fold increase in fluorescence, whilst displaying tumor cell selectivity in phototoxicity.

Although a dual uptake of carrier and drug would be anticipated, the similarity in action observed of the conjugates to the free drug means it is possible that extra and/or intracellular separation of the drug from the polymer occurs. However, no direct evidence from the current study could enlighten upon this situation at the current moment in time and thus the precise mechanistic details of the uptake and any possible release of the conjugates are a matter of future investigation.

### Acknowledgements

Thanks to Dr Mario Waser and Dr Beate Hager of the Institute for Organic Chemistry, Johannes Kepler University, Linz, Austria for providing the synthetic hypericin used for polymer conjugation. We also thank Dr Andreas Kubin (Planta Natural Products, Vienna, Austria) for providing pristine hypericin as a reference in spectrophotometry.

## References

- 1 P. Agostinis, A. Vantieghem, W. Merlevede and P. A. de Witte. Hypericin in cancer treatment: more light on the way. *Int J Biochem Cell Biol*, 2002, **34**, 221.
- 2 M. Alecu, C. Ursaciuc, F. Halalau, G. Coman, W. Merlevede, E. Waelkens and P. de Witte. Photodynamic treatment of basal cell carcinoma and squamous cell carcinoma with hypericin. *Anticancer Res*, 1998, **18**, 4651.
- 3 M. Blank, G. Kostenich, G. Lavie, S. Kimel, Y. Keisari and A. Orenstein. Wavelength-dependent properties of photodynamic therapy using hypericin in vitro and in an animal model. *Photochem Photobiol*, 2002, **76**, 335.
- 4 I. Cavarga, P. Brezani, M. Cekanova-Figurova, P. Solar, P. Fedorocko and P. Miskovsky. Photodynamic therapy of murine fibrosarcoma with topical and systemic administration of hypericin. *Phytomedicine*, 2001, **8**, 325.
- 5 C. S. Head, Q. Luu, J. Sercarz and R. Saxton. Photodynamic therapy and tumor imaging of hypericin-treated squamous cell carcinoma. *World J Surg Oncol*, 2006, **4**, 87.
- 6 M. Olivo, H. Y. Du and B. H. Bay. Hypericin lights up the way for the potential treatment of nasopharyngeal cancer by photodynamic therapy. *Curr Clin Pharmacol*, 2006, **1**, 217.
- 7 R. Sanovic, T. Verwanger, A. Hartl and B. Krammer. Low dose hypericin-PDT induces complete tumor regression in BALB/c mice bearing CT26 colon carcinoma. *Photodiagnosis Photodyn Ther*, 2011, **8**, 291.
- 8 C. L. Saw, M. Olivo, K. C. Soo and P. W. Heng. Delivery of hypericin for photodynamic applications. *Cancer Lett*, 2006, **241**, 23.
- 9 P. S. P. Thong, M. Olivo, W. W. L. Chin, R. Bhuvanewari, K. Mancner and K. C. Soo. Clinical application of fluorescence endoscopic imaging using hypericin for the diagnosis of human oral cavity lesions. *British Journal of Cancer*, 2009, **101**, 1580.
- 10 I. Zupko, A. R. Kamuhabwa, M. A. D'Hallewin, L. Baert and P. A. De Witte. In vivo photodynamic activity of hypericin in transitional cell carcinoma bladder tumors. *Int J Oncol*, 2001, **18**, 1099.
- 11 V. Engelhardt, B. Krammer and K. Plaetzer. Antibacterial photodynamic therapy using water-soluble formulations of hypericin or mTHPC is effective in inactivation of *Staphylococcus aureus*. *Photochem Photobiol Sci*, 2010, **9**, 365.
- 12 A. Karioti and A. R. Bilia. Hypericins as potential leads for new therapeutics. *Int J Mol Sci*, 2010, **11**, 562.
- 13 B. Krammer and T. Verwanger. Molecular response to hypericin-induced photodamage. *Curr Med Chem*, 2012, **19**, 793.
- 14 E. Buytaert, J. Y. Matroule, S. Durinck, P. Close, S. Kocanova, J. R. Vandenneede, P. A. de Witte, J. Piette and P. Agostinis. Molecular effectors and modulators of hypericin-mediated cell death in bladder cancer cells. *Oncogene*, 2008, **27**, 1916.
- 15 M. Zeisser-Labouebe, N. Lange, R. Gurny and F. Delie. Hypericin-loaded nanoparticles for the photodynamic treatment of ovarian cancer. *International Journal of Pharmaceutics*, 2006, **326**, 174.
- 16 A. Huygens, A. R. Kamuhabwa and P. A. de Witte. Stability of different formulations and ion pairs of hypericin. *Eur J Pharm Biopharm*, 2005, **59**, 461.
- 17 A. S. Derycke and P. A. De Witte. Transferrin-mediated targeting of hypericin embedded in sterically stabilized PEG-liposomes. *Int J Oncol*, 2002, **20**, 181.
- 18 A. Kubin, P. Meissner, F. Wierrani, U. Burner, A. Bodenteich, A. Pytel and N. Schmeller. Fluorescence diagnosis of bladder cancer with new water soluble hypericin bound to polyvinylpyrrolidone: PVP-hypericin. *Photochem Photobiol*, 2008, **84**, 1560.
- 19 M. Van De Putte, T. Roskams, G. Bormans, A. Verbruggen and P. A. De Witte. The impact of aggregation on the biodistribution of hypericin. *Int J Oncol*, 2006, **28**, 655.
- 20 A. Kubin, H. G. Loew, U. Burner, G. Jessner, H. Kolbabeck and F. Wierrani. How to make hypericin water-soluble. *Pharmazie*, 2008, **63**, 263.

- 21 J. Vandepitte, B. Van Cleynenbreugel, K. Hettinger, H. Van Poppel and P. A. de Witte. Biodistribution of PVP-hypericin and hexaminolevulinat-induced PpIX in normal and orthotopic tumor-bearing rat urinary bladder. *Cancer Chemother Pharmacol*, 2011, **67**, 775.
- 22 J. Vandepitte, M. Roelants, B. Van Cleynenbreugel, K. Hettinger, E. Lerut, H. Van Poppel and P. A. de Witte. Biodistribution and photodynamic effects of polyvinylpyrrolidone-hypericin using multicellular spheroids composed of normal human urothelial and T24 transitional cell carcinoma cells. *J Biomed Opt*, 2011, **16**, 018001.
- 23 R. Duncan. Polymer therapeutics as nanomedicines: new perspectives. *Current Opinion in Biotechnology*, 2011, **22**, 492.
- 24 R. Duncan and S. C. Richardson. Endocytosis and intracellular trafficking as gateways for nanomedicine delivery: opportunities and challenges. *Mol Pharm*, 2012, **9**, 2380.
- 25 E. Markovsky, H. Baabur-Cohen, A. Eldar-Boock, L. Omer, G. Tiram, S. Ferber, P. Ofek, D. Polyak, A. Scomparin and R. Satchi-Fainaro. Administration, distribution, metabolism and elimination of polymer therapeutics. *Journal of Controlled Release*, 2012, **161**, 446.
- 26 R. Gaspar and R. Duncan. Polymeric carriers: preclinical safety and the regulatory implications for design and development of polymer therapeutics. *Adv Drug Deliv Rev*, 2009, **61**, 1220.
- 27 V. Bühler. Polyvinylpyrrolidone Excipients for Pharmaceuticals. 2005.
- 28 H. A. Ravin, A. M. Seligman and J. Fine. Polyvinyl Pyrrolidone as a Plasma Expander. *New England Journal of Medicine*, 1952, **247**, 921.
- 29 H. R. Allcock and N. L. Morozowich. Bioerodible polyphosphazenes and their medical potential. *Polymer Chemistry*, 2012, **3**, 578.
- 30 A. Andrianov. Water-Soluble Polyphosphazenes for Biomedical Applications. *Journal of Inorganic and Organometallic Polymers and Materials*, 2006, **16**, 397.
- 31 I. Teasdale, S. Wilfert, I. Nischang and O. Brüggemann. Multifunctional and biodegradable polyphosphazenes for use as macromolecular anti-cancer drug carriers. *Polymer Chemistry*, 2011, **2**, 828.
- 32 H. Henke, S. Wilfert, A. Iturmendi, O. Brüggemann and I. Teasdale. Branched polyphosphazenes with controlled dimensions. *Journal of Polymer Science Part A: Polymer Chemistry*, 2013, **51**, 4467.
- 33 I. Teasdale and O. Brüggemann. Polyphosphazenes: Multifunctional, Biodegradable Vehicles for Drug and Gene Delivery. *Polymers*, 2013, **5**, 161.
- 34 S. Wilfert, A. Iturmendi, W. Schoefberger, K. Kryeziu, P. Heffeter, W. Berger, O. Brüggemann and I. Teasdale. Water-soluble, biocompatible polyphosphazenes with controllable and pH-promoted degradation behavior. *Journal of Polymer Science Part A: Polymer Chemistry*, 2014, **52**, 287.
- 35 H. Falk, J. Meyer and M. Oberreiter. A Convenient Semisynthetic Route to Hypericin. *Monatshefte Fur Chemie*, 1993, **124**, 339.
- 36 A. K. Andrianov, A. Marin and P. Peterson. Water-Soluble Biodegradable Polyphosphazenes Containing N-Ethylpyrrolidone Groups. *Macromolecules*, 2005, **38**, 7972.
- 37 I. Teasdale, M. Waser, S. Wilfert, H. Falk and O. Brüggemann. Photoreactive, water-soluble conjugates of hypericin with polyphosphazenes. *Monatshefte Fur Chemie*, 2012, **143**, 355.
- 38 Y. F. Ho, M. H. Wu, B. H. Cheng, Y. W. Chen and M. C. Shih. Lipid-mediated preferential localization of hypericin in lipid membranes. *Biochim Biophys Acta*, 2009, **1788**, 1287.
- 39 J. Knaup. Treatment of squamous cell carcinoma of epidermolysis bullosa patients by photodynamic therapy: in in-vitro study. Master thesis, University of Salzburg, 2008.
- 40 A. L. Vandenberghe, E. M. Delaey, A. M. Vantieghem, B. E. Himpens, W. J. Merlevede and P. A. de Witte. Cytotoxicity and antiproliferative effect of hypericin and derivatives after photosensitization. *Photochem Photobiol*, 1998, **67**, 119.

- 41 M. Blank, M. Mandel, S. Hazan, Y. Keisari and G. Lavie. Anti-cancer activities of hypericin in the dark. *Photochem Photobiol*, 2001, **74**, 120.
- 42 P. Agostinis, A. Donella-Deana, J. Cuveele, A. Vandenberghe, S. Sarno, W. Merlevede and P. de Witte. A comparative analysis of the photosensitized inhibition of growth-factor regulated protein kinases by hypericin-derivatives. *Biochem Biophys Res Commun*, 1996, **220**, 613.
- 43 M. Blank, G. Lavie, M. Mandel, S. Hazan, A. Orenstein, D. Meruelo and Y. Keisari. Antimetastatic activity of the photodynamic agent hypericin in the dark. *Int J Cancer*, 2004, **111**, 596.
- 44 V. Huntosova, D. Buzova, D. Petrovajova, P. Kasak, Z. Nadova, D. Jancura, F. Sureau and P. Miskovsky. Development of a new LDL-based transport system for hydrophobic/amphiphilic drug delivery to cancer cells. *Int J Pharm*, 2012, **436**, 463.
- 45 R. Penjweini, N. Smisdom, S. Deville and M. Ameloot. Transport and accumulation of PVP-Hypericin in cancer and normal cells characterized by image correlation spectroscopy techniques. *Biochim Biophys Acta*, 2014, **1843**, 855.
- 46 I. G. England, L. Naess, R. Blomhoff and T. Berg. Uptake, intracellular transport and release of <sup>125</sup>I-poly(vinylpyrrolidone) and [<sup>14</sup>C]-sucrose-asialofetuin in rat liver parenchymal cells. Effects of ammonia on the intracellular transport. *Biochem Pharmacol*, 1986, **35**, 201.
- 47 A. P. Castano, T. N. Demidova and M. R. Hamblin. Mechanisms in photodynamic therapy: part one - photosensitizers, photochemistry and cellular localization. *Photodiagnosis and Photodynamic Therapy*, 2004, **1**, 279.
- 48 D. Kessel, Y. Luo, P. Mathieu and J. J. Reiners, Jr. Determinants of the apoptotic response to lysosomal photodamage. *Photochem Photobiol*, 2000, **71**, 196.
- 49 U. Repnik, V. Stoka, V. Turk and B. Turk. Lysosomes and lysosomal cathepsins in cell death. *Biochim Biophys Acta*, 2012, **1824**, 22.
- 50 E. Buytaert, G. Callewaert, N. Hendrickx, L. Scorrano, D. Hartmann, L. Missiaen, J. R. Vandenheede, I. Heirman, J. Grooten and P. Agostinis. Role of endoplasmic reticulum depletion and multidomain proapoptotic BAX and BAK proteins in shaping cell death after hypericin-mediated photodynamic therapy. *Faseb J*, 2006, **20**, 756.
- 51 M. Shi, T. Zhang, L. Sun, Y. Luo, D. H. Liu, S. T. Xie, X. Y. Song, G. F. Wang, X. L. Chen, B. C. Zhou and Y. Z. Zhang. Calpain, Atg5 and Bak play important roles in the crosstalk between apoptosis and autophagy induced by influx of extracellular calcium. *Apoptosis*, 2013, **18**, 435.
- 52 Z. Jiang, Z. Hu, L. Zeng, W. Lu, H. Zhang, T. Li and H. Xiao. The role of the Golgi apparatus in oxidative stress: is this organelle less significant than mitochondria? *Free Radic Biol Med*, 2011, **50**, 907.
- 53 R. Ritz, F. Roser, N. Radomski, W. S. Strauss, M. Tatagiba and A. Gharabaghi. Subcellular colocalization of hypericin with respect to endoplasmic reticulum and Golgi apparatus in glioblastoma cells. *Anticancer Res*, 2008, **28**, 2033.
- 54 J. Berlanda, T. Kiesslich, C. B. Oberdanner, F. J. Obermair, B. Krammer and K. Plaetzer. Characterization of apoptosis induced by photodynamic treatment with hypericin in A431 human epidermoid carcinoma cells. *J Environ Pathol Toxicol Oncol*, 2006, **25**, 173.
- 55 V. Sackova, P. Fedorocko, B. Szilardiova, J. Mikes and J. Kleban. Hypericin-induced photocytotoxicity is connected with G2/M arrest in HT-29 and S-phase arrest in U937 cells. *Photochem Photobiol*, 2006, **82**, 1285.
- 56 H. B. Lee, A. S. Ho and S. H. Teo. p53 Status does not affect photodynamic cell killing induced by hypericin. *Cancer Chemother Pharmacol*, 2006, **58**, 91.
- 57 J. Mikes, J. Koval, R. Jendzelovsky, V. Sackova, I. Uhrinova, M. Kello, L. Kulikova and P. Fedorocko. The role of p53 in the efficiency of photodynamic therapy with hypericin and subsequent long-term survival of colon cancer cells. *Photochem Photobiol Sci*, 2009, **8**, 1558.
- 58 X. Wang, Y. Guo, S. Yang, C. Wang, X. Fu, J. Wang, Y. Mao, J. Zhang and Y. Li. Cellular and molecular mechanisms of photodynamic hypericin therapy for nasopharyngeal carcinoma cells. *J Pharmacol Exp Ther*, 2010, **334**, 847.

